The Application of Ultrasonic Locating Techniques to Ophthalmology

II. Ultrasonic Slit Lamp in the Ultrasonic Visualization of Soft Tissues

GILBERT BAUM, M.D., Port Chester, N. Y., and IVAN GREENWOOD, B.S., Pleasantville, N. Y.

Introduction

This is a preliminary report of the visualization of the interior of the light-opaque eye and the retro-ocular areas by pulsed ultrasonic echographic methods. Non-radio-opaque foreign materials, such as wood and plastics, may also be visualized, as well as soft tissue pathology.

At present no other method can yield the information obtained by the technique to be described. A comparison of the visual appearance of a normal beef eye, the x-ray appearance, and the sonic appearance graphically illustrates this contention (Fig. 1). The x-ray demonstrates only the gross outline of the eye. The ultrasonogram reveals a cross section of the internal structure of the eye equivalent in detail to a low-power photomicrograph. Serial ultrasonic tomograms (Figs. 13 to 21) yield a composite picture of the eye at all levels without in any way altering the tissues.

Precise direct measurement of the depth within the tissue is possible with this device. This dimension could not heretofore be directly measured short of surgical exposure.

In the past, soft tissue structures within the body could be visualized only by surgical exploration and soft tissue x-ray techniques with the use of the contrast media.

Disadvantages of X-Ray Techniques

X-ray visualization of soft tissue possesses inherent disadvantages because the

This project was supported by Grant B-993 (C) from the National Institutes of Health, Bethesda, Md., and the Veterans' Administration Hospital, Bronx.

Clinical Assistant in Ophthalmology, New York University Post-Graduate Medical School (Dr. Baum); Assistant Director of Research, Avionics Division, General Precision Laboratory, Pleasantville, N. Y. (Mr. Greenwood).

Fig. 1.—A comparison of the appearance of the beef eye grossly, by x-ray, and ultrasonographically. *A*, gross appearance. *B*, x-rays, anteroposterior and lateral. *C*, ultrasonic tomograph.

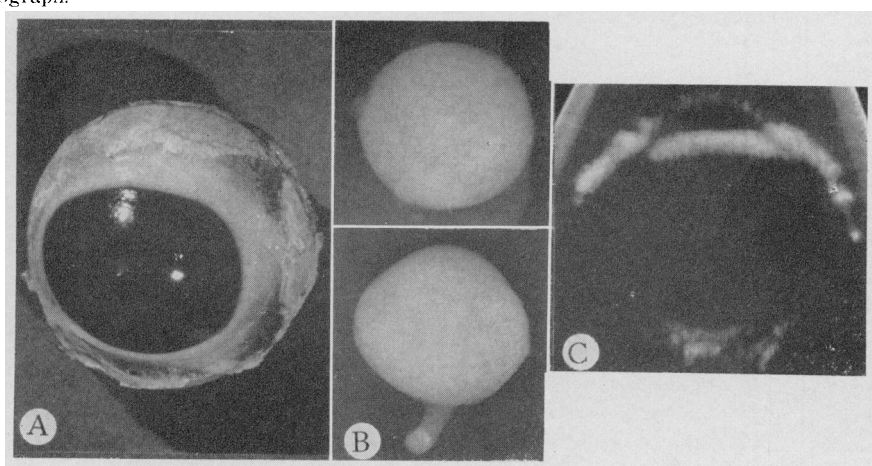

Summary of Advantages of Ultrasonic Visualization

Advantages of Ultrasonic Visualization of Soft Tissues	Disadvantages of X-Ray Visualization of Soft Tissues
1. The soft tissues may be visualized directly, without the use of contrast media; the detail is equivalent to that of a low-power photomicrograph	1. Soft tissues have uniform density to x-ray; contrast media are required, but the detail fails to equal that obtained by ultrasonic visualization; contrast media are irritating and possess toxic side-effects
2. Safe at the levels used for visualization; no immediate, cumulative or delayed effects	2. Danger of x-ray exposure and cumulative effects
3. Depth and angular location can be directly measured, without markers	3. Markers are required
4. Most forms of foreign materials may be visualized and localized	4. Many substances possess the same x-ray density as the soft tissues in which they are embedded and cannot be visualized
5. Visualization and localization may be performed in any part of the eye or orbit	5. Radioisotope localization and identification of tumors is dependent upon their anterior location and selective uptake

soft tissues of the body exhibit a uniform density on x-ray examination. Even the best soft tissue x-ray techniques demonstrate only gross soft tissue structure (Fig. 1).

Contrast media, such as iodides, barium, and air, have been used to obtain a greater density differential and delineate the finer defects in soft tissue structure. At best, these fail to provide the detail available by ultrasonic visualization.

Such media used intraorbitally have proven to be irritable.[1] Walsh[2] has reported numerous complications following carotid angiography.

Tumor localization by radioisotope-uptake may be unsatisfactory because lesions of the posterior segment of the eye are inaccessible to the Geiger counter and/or the tumors fail to exhibit a selective uptake of the radioisotope.[3]

All forms of x-ray subject the eye and body to the hazard of exposure, as well as the cumulative and delayed action of x-ray.

Advantages of Ultrasonic Visualization

The soft tissues themselves can be "visualized" by high-frequency sound waves. Thus, the need for contrast media is eliminated. Ultrasonic waves are harmless at the energy levels used to visualize soft tissues. Doses 1000 times in excess of those used in the ultrasonic locator are without demonstrable effect upon the tissues at reduced peak voltages. There is no known delayed or cumulative damage from ultrasonic radiation, such as may follow x-ray. All portions of the globe and orbit may be reached. Selective uptake by various tissues is not a problem, but differences in the reflective and absorptive properties of tissues in relation to ultrasonic waves may actually facilitate the differential diagnosis of tissues. (This phase of ultrasonic differentiation will be discussed in another paper.)

Principle of Operation

An ultrasonic locator is essentially a slit lamp in which pulsed high-frequency sound waves have been substituted for the light source. A microphone is substituted for the microscope. The entire assembly scans the eye so as to obtain a cross sectional view (i. e., a tomogram) of the tissue being studied. In practice, considerable simplification of the apparatus is achieved by combining the sound-generating and -receiving source into one unit, called the transducer.

Analysis of Operation

Figure 2 is a block diagram of the major units of the ultrasonic locator. An electrical pulse is produced by the generator (*A*). This pulse causes the crystal to produce a pulse of high-frequency sound waves (*B*). The latter must be coupled to the eye by a liquid to prevent their absorption by the air.

How Tissues Are Visualized

Figure 3 is a representation of what happens at the eye when both light and sound are used.

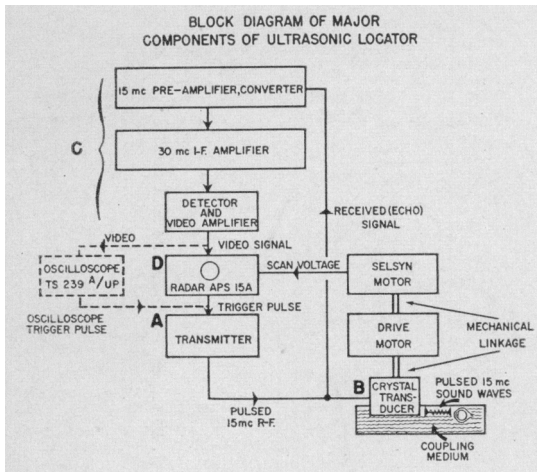

Figure 2

Fig. 2.—Block diagram of major components of ultrasonic locator. *A*, pulsed 15 mc. R-F current generated by transmitter. *B*, crystal converts electrical energy into sound. Sound waves travel through water and strike the tissue. Reflected sound waves received back at crystal, which reconverts the sound back into electrical impulses. *C*, electrical impulses are amplified by receiver. *D*, radar receiver converts electrical impulses into blobs of light of proportional intensity and correct position.

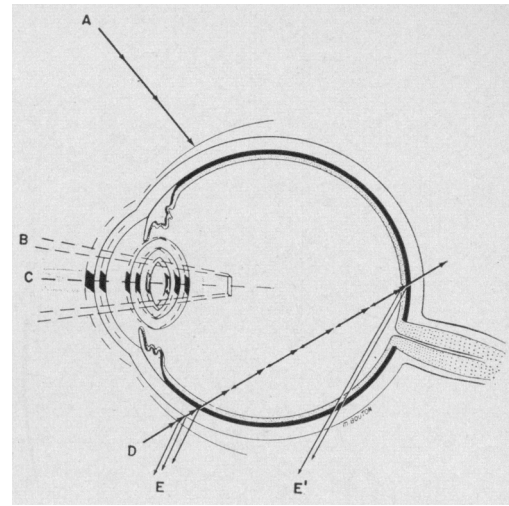

Figure 3

Fig. 3.—A comparison of the visualization of the eye by the light and sonic slit lamps. *A*, light incident upon the heterogeneous surface of the sclera is absorbed, diffused, and reflected so that only the surface of the sclera can be seen. *B*, light incident upon the homogeneous cornea is transmitted into the depths of the eye. *C*, as light passes through zones of optical discontinuity, i. e., different indices of refraction, a reflection occurs at each interface. *D*, high-frequency sound waves can penetrate the soft tissues of the body regardless of their optical properties. *E* and *E'*, as the sound waves pass through tissues possessing different acoustic impedances, reflections are set up at each interface. These reflections are detected by the receiving crystal and converted into electrical impulses. The latter are amplified and then converted into light of varying intensities, so as to form a picture on the face of the cathode-ray tube.

When the sound pulse (Fig. 3*D*) strikes any surface of the eye, a portion of the sound wave is reflected and the remainder is transmitted to the deeper structures of the eye. As the sound waves pass through tissues of different acoustic impedances a portion of the sound energy is reflected (Fig. 3*E* and *E'*) and the remainder is transmitted onward, until the energy is totally absorbed. A reflected wave is set up at each interface. An identical phenomenon occurs optically as the light beam of the slit lamp traverses tissues whose index of refraction differs (Fig. 3*B* and *C*). The outstanding difference is that the structures which are opaque to light, such as the sclera and the retro-ocular areas, are transparent to sound.

Methods of Presenting the Information

The reflected sound waves are picked up by the microphone, which converts the

Fig. 4.—Formation of the ultrasonogram. *A*, the appearance of the front and rear surfaces without scanning (trace off). *B*, appearance of front and rear surfaces with a slow scan (trace off). *C*, formation of the ultrasonogram with use of a rapid scan (trace on).

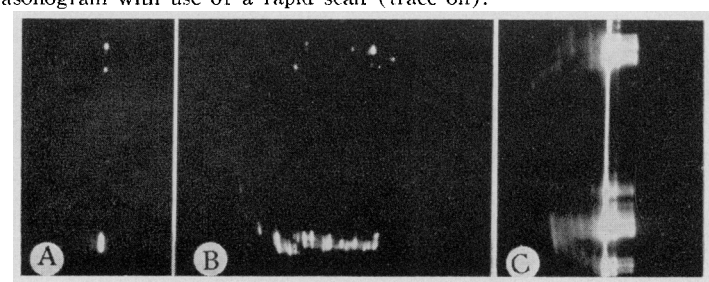

sound energy into electrical impulses (Fig. 2*B*). The electrical impulses are amplified (Fig. 2*C*) and then converted into blobs of light on an oscilloscope in which the intensity is proportional to the intensity of the reflected sound (Figs. 2*D* and 4*A*).

To obtain a cross sectional view of the tissues under study, the transducer is moved across these tissues (Fig. 4*B*). A mechanical-electrical linkage system correlates the position of the electrical trace of the oscilloscope with that of the transducer so that a picture, or sonogram, results. Figure 4*C* shows the formation of the ultrasonogram; the outlines can be seen dimly, and the trace line is prominent.

Technique of Using the Sonic Slit Lamp

Experimental studies are conducted by submerging the tissues and transducer in a tank of saline or water (Fig. 5). Examination of patients is conducted by mounting the transducer on an adjustable assembly such as is shown in Figure 6. The patient places his face inside a rubber mask built into the side of the tank. The tank is filled with isotonic saline.

Fig. 5.—Detailed view of scanning system. *A*, Selsyn motor, for synchronous positioning of transducer and sweep of cathode-ray tube. *B*, drive motor. *C*, transducer, mounted at the end of the shaft of the Selsyn motor. *D*, tank for submerging specimens and transducer.

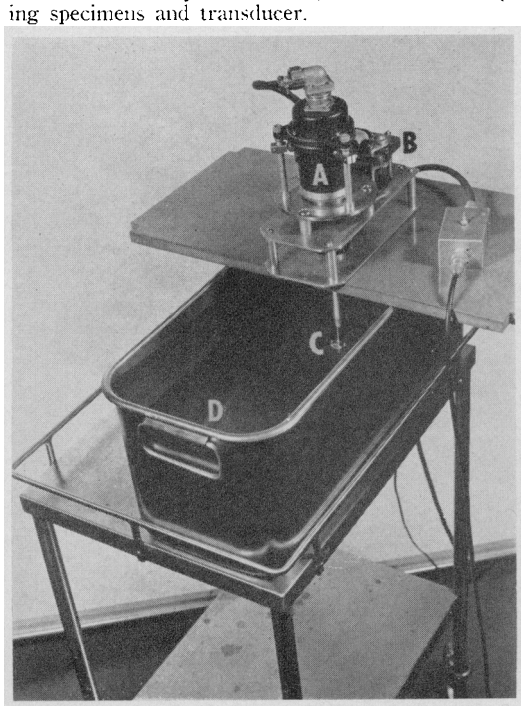

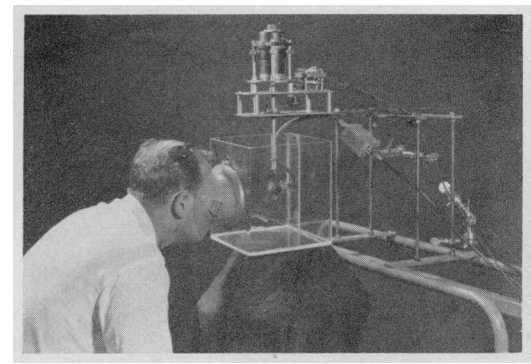

Fig. 6.—Apparatus used for the clinical examination of patients.

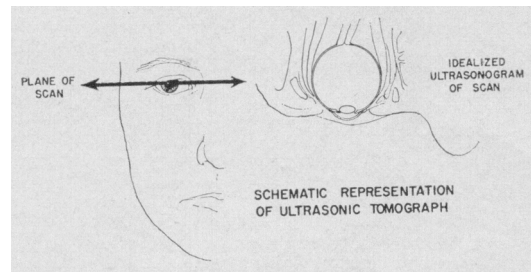

Fig. 7.—Schematic representation of an ultrasonic tomogram. Serial tomography is performed by scanning the eye at succeeding levels.

Orientation

The schematic diagram (Fig. 7) facilitates the understanding of the succeeding ultrasonograms. The ultrasonogram represents a horizontal section, or planigram, through a level of the eye. It is similar to a slit-lamp section, except that only tissues in the section are visualized. The remainder of the eye can only be visualized by performing serial planigrams at other levels.

Fig. 8.—Gross appearance of the eyes of the patient. Note the haziness of the cornea and the hyphema of the right eye.

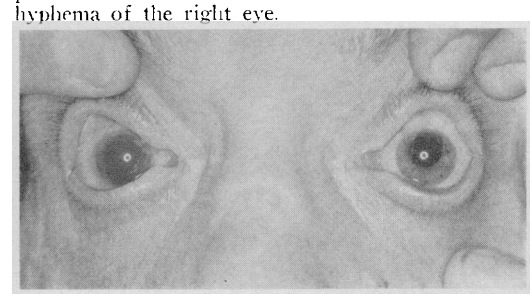

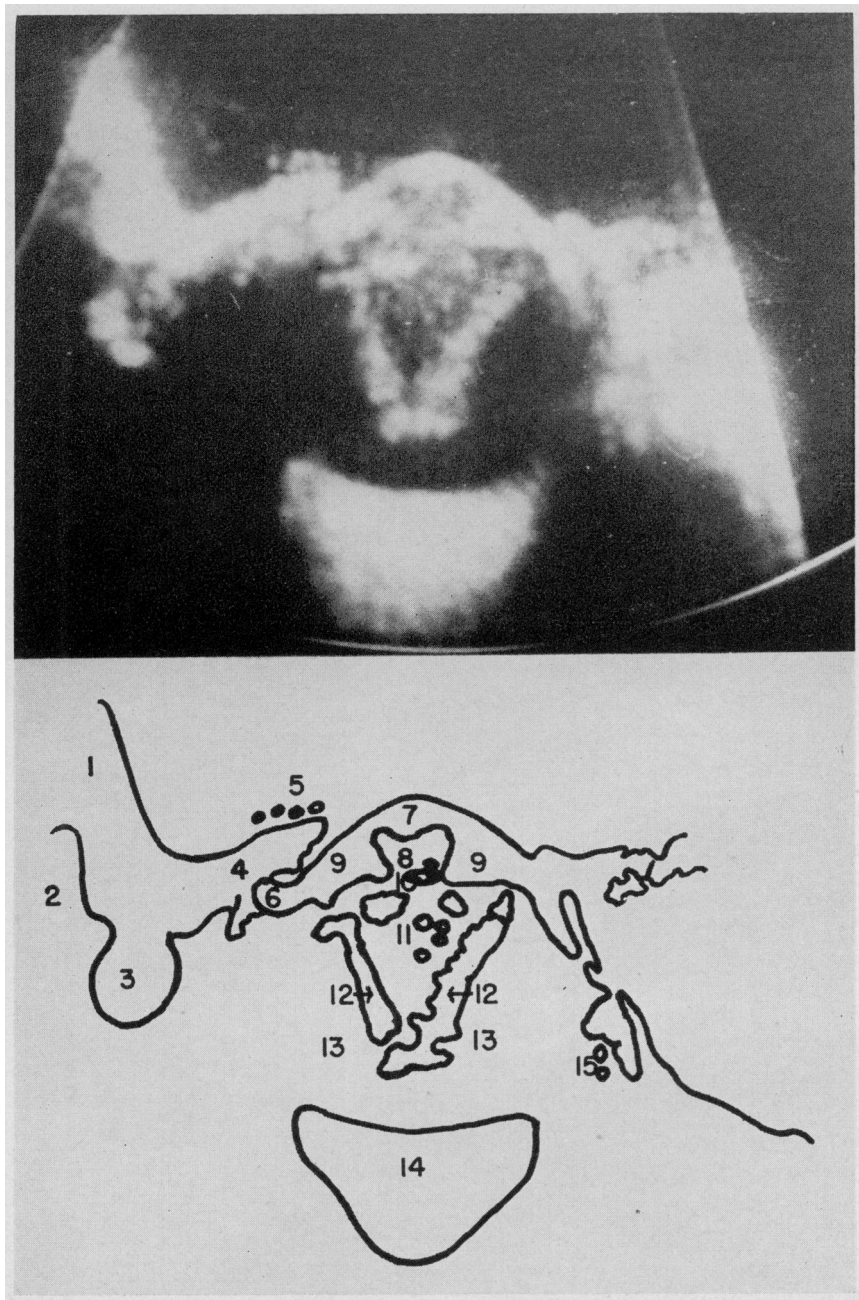

Fig. 9.—Echogram of the right eye, in situ, of patient in Figure 8. *1*, nose; *2*, nasal cavity; *3*, nasolacrimal sac; *4*, lid; *5*, cilia; *6*, caruncle; *7*, cornea; *8*, anterior chamber containing blood; *9*, ciliary body; *10*, iris; *11*, vitreous hemorrhage contained wholly within the totally detached retina; *12*, totally detached retina; *13*, clear subretinal fluid; *14*, sclera and retro-orbital fat.

The term "sections" is thus used in the same sense as in "slit-lamp section." An ultrasonic tomogram or planigram would be a more descriptive and accurate term. The ultrasonograms appear as compound coronal-sagittal sections, as viewed from an anterior position.

Fields of Application

The commonest use for the sonic slit lamp is the visualization of the light-opaque eye, e. g., in cases of opacification due to corneal opacification, cataract, or vitreous hemorrhage or exudate. The following cases will demonstrate the diagnostic poten-

tials of this instrument. At present no other device can divulge the information obtainable with this device.

Differential Diagnosis in Complicated Retinal Detachments.—Diagnosis in retinal detachment is frequently complicated by semiopaque or totally opaque refractive media or by the presence of a tumor or radiolucent foreign body.

Figure 8 shows the eyes of a patient with corneal edema, hyphema, surgical aphakia, and a massive vitreous hemorrhage (no

Fig. 10.—This figure best demonstrates the lateral check ligament (*11*) and the passage of the optic nerve (*9*) into the orbital fat. *1*, lid; *2*, cilia; *3*, cornea; *4*, anterior chamber; *5*, iris; *6*, ciliary body; *7*, vitreous bands and hemorrhage; *8*, detached retina; *9*, passage of optic nerve through sclera into the orbit; *10* orbital fat; *11*, check ligament of the lateral rectus muscle.

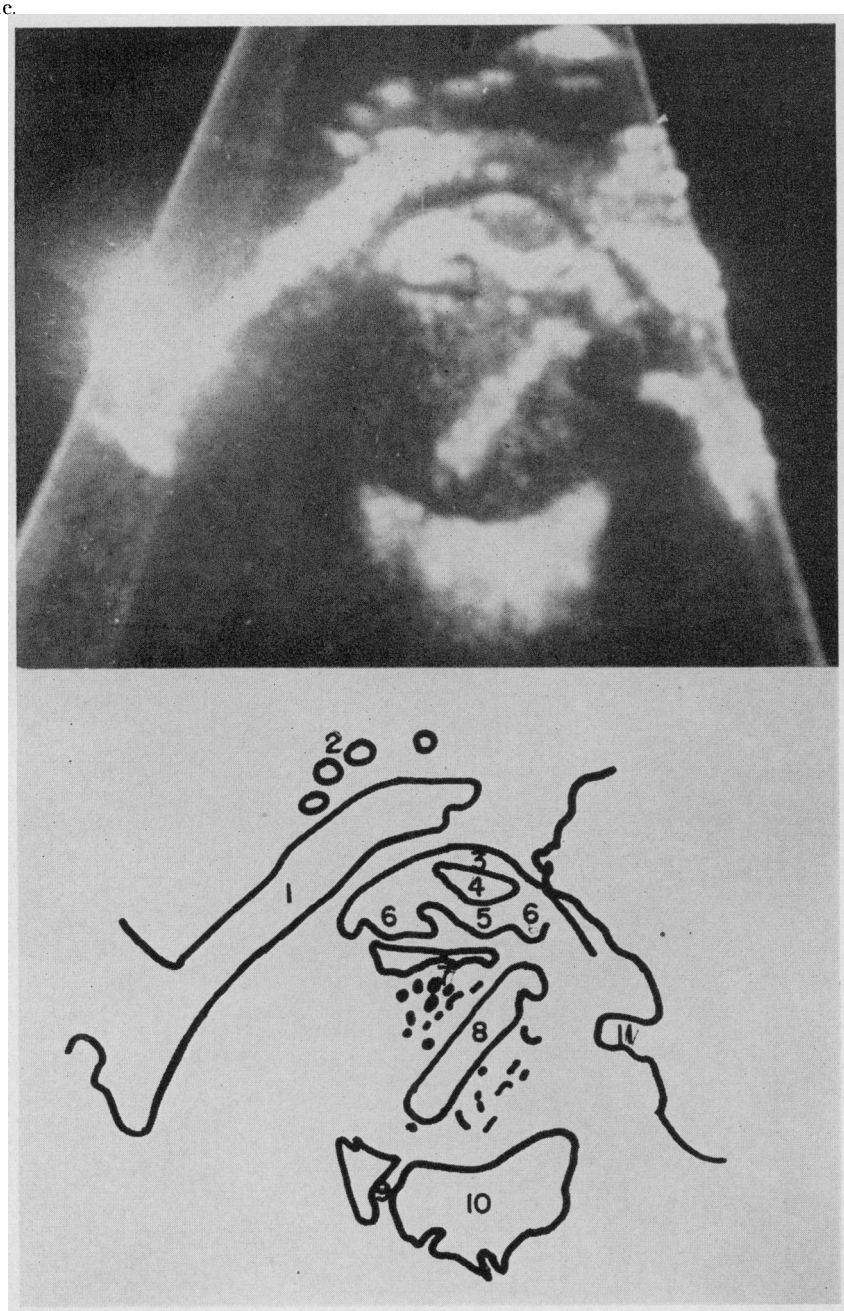

fundus reflex), which made it impossible to visualize the fundus.*

*Drs. A. Haft and M. Bernstein, of the Ophthalmology Service, Bronx Veterans' Administration Hospital, referred this patient and supplied the clinical data.

An ultrasonogram of the area (Fig. 9) prior to enucleation of the eye demonstrated the above findings. In addition, the sonogram demonstrated that the retina was wholly detached and that the vitreous hemorrhage was contained within the detached

Fig. 11.—The lateral rectus muscle is visualized at (12). *1*, nose; *2*, nasal cavity; *3*, nasolacrimal sac; *4*, caruncle; *5*, cornea; *6*, anterior chamber; *7*, ciliary body; *8*, iris; *9*, vitreous hemorrhage and bands; *10*, detached retina; *11*, orbital fat; *12*, lateral rectus muscle at level of the posterior pole of the eye.

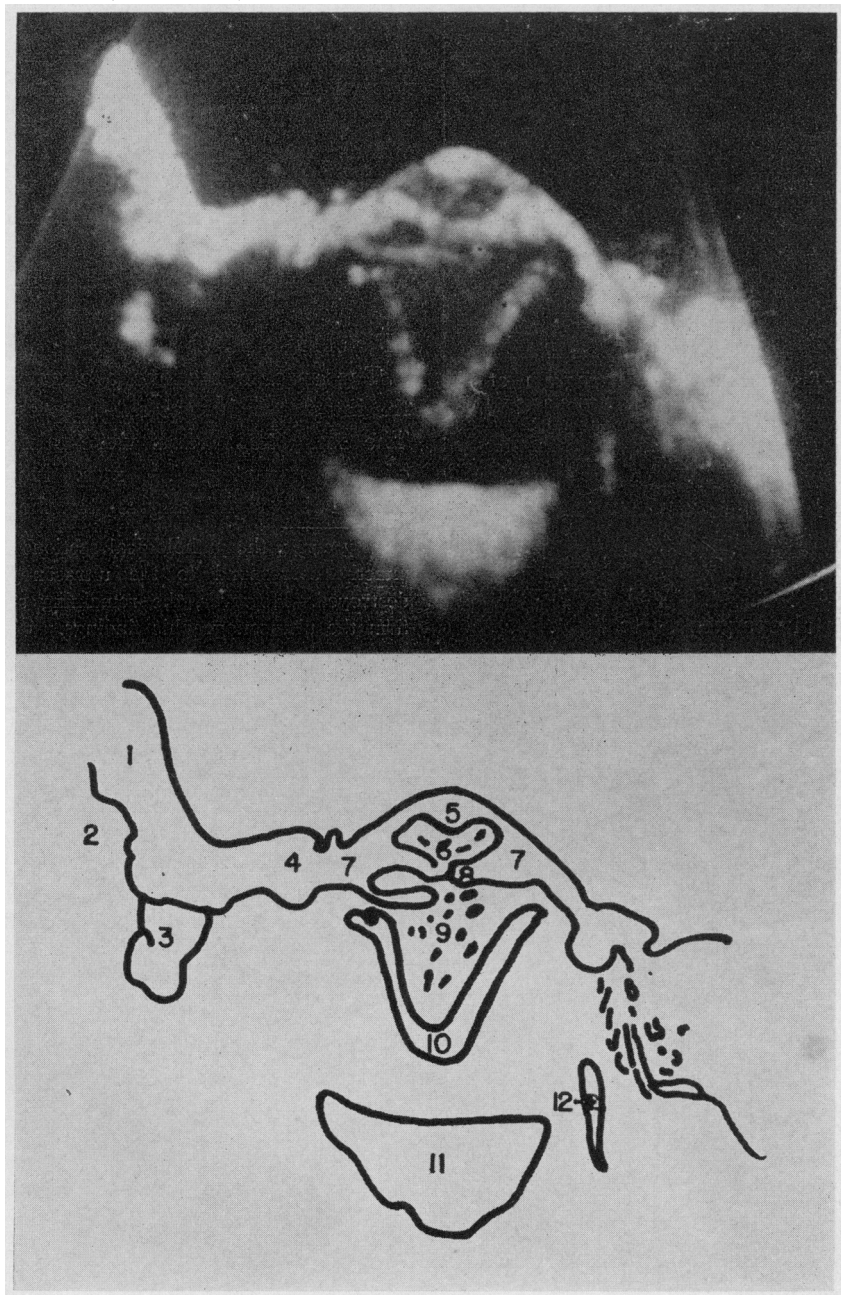

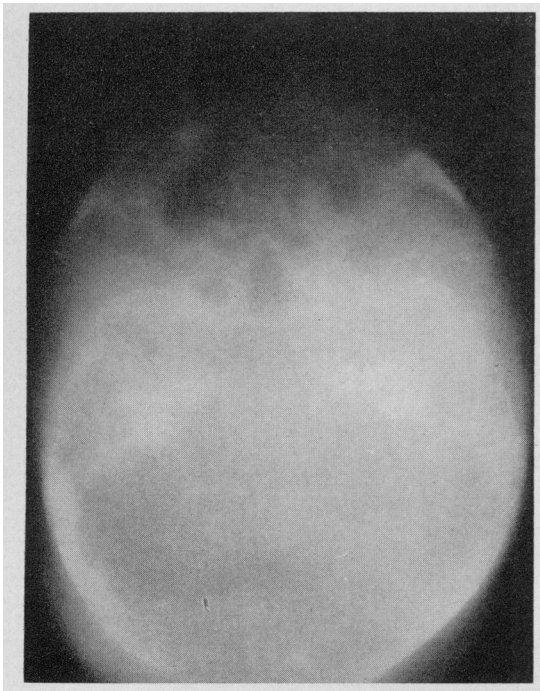

Fig. 12.—Transverse x-ray tomogram at the level of the superior and middle turbinates of the nasal cavity. Note the complete absence of any soft tissue detail within the orbits. (Drs. Bernard Roswit and Sol Ungar, of the radioisotope section, Bronx Veterans' Administration Hospital, furnished this tomogram, as well as its interpretation.)

retina. The subretinal fluid was relatively clear. This pathology was visualized despite the total opaqueness to light.

The nasolacrimal sac, the optic nerve and the orbital fat about it, and the check ligament of the lateral rectus muscle are well visualized in Figure 10. The intraorbital portion of the lateral rectus muscle in the area of the posterior pole of the eye is demonstrated in Figure 11. This interpretation is based on the normal anatomy of the area.

Figure 12 is an x-ray tomogram of the orbit. The greater clarity and definition of the soft tissues in the ultrasonic tomogram are evident upon simple comparison.

After enucleation, serial ultrasonic tomograms were made. These demonstrated total retinal detachment and the relative position of the retina at different levels within the eye. Serial tissue sections through approximately the same areas of the globe confirmed the ultrasonograms (Figs. 13 to 21).†

These sonic sections are made through the intact eye, just as slit-lamp sections are. The sonic tomograms were taken in steps of approximately 1.5 mm. from top to bottom at right angles to the anterior-

† By error, the pathological sections which more exactly correspond to the ultrasonograms were destroyed. However, the remaining sections confirm the ultrasonographic findings.

Fig. 13.—Figures 13 to 21 show serial ultrasonic tomograms of the enucleated eye of the patient in Figure 8. Note the change in the position of the retina at different levels through the eye.

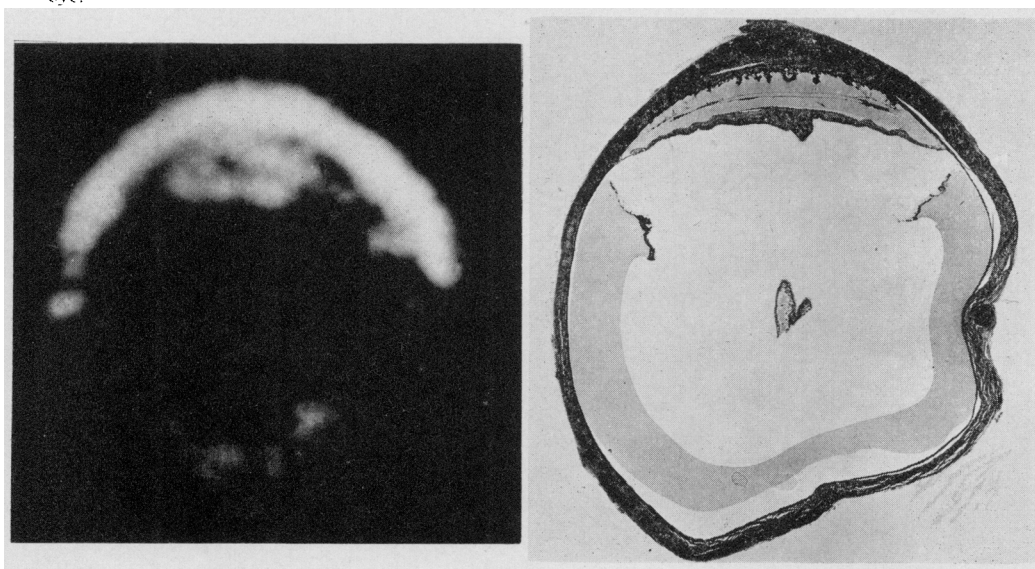

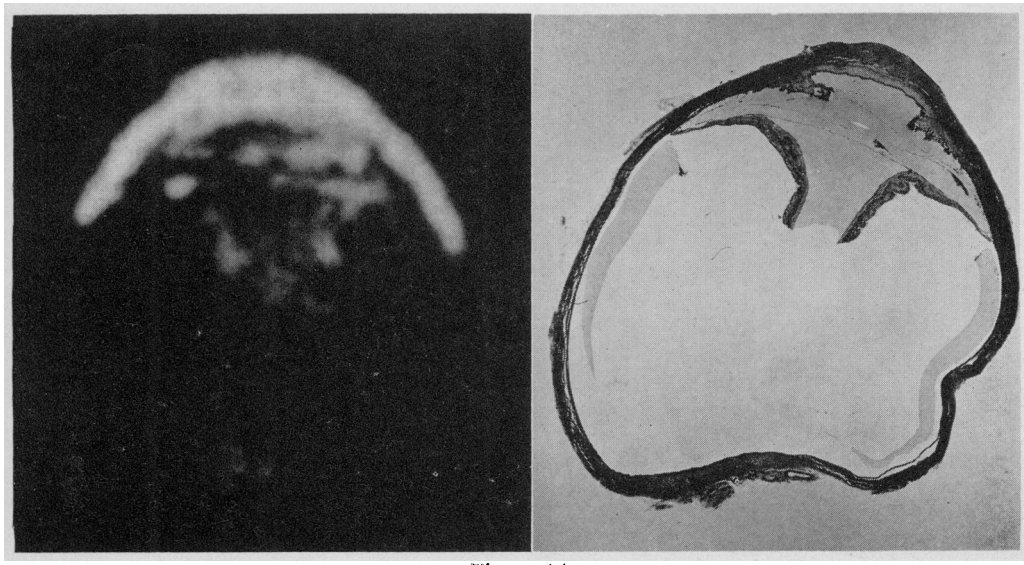

Figure 14

posterior axis, i. e., in both the sagittal and corneal planes.

Figure 16 implies that the vitreous bands may be visualized with the locator. The bands in this section were vascularized, which may account for their visualization. Further study of this point is necessary.

The sections in Figures 14 to 20 exhibited the following pathology: neovascularization and scarring of the cornea, hyphema, anterior synechiae which formed a false angle, entropion of the iris with connective tissue strands radiating to the ciliary body, hemorrhage about the ciliary body, vitreous bands and hemorrhages, total retinal detachment, and clear subretinal fluid. The sections in Figures 13 and 21 were cut above and below the cornea, and so none of the anterior chamber pathology appears in these sections.

Vitreous Hemorrhage. The criteria which differentiates a simple vitreous hem-

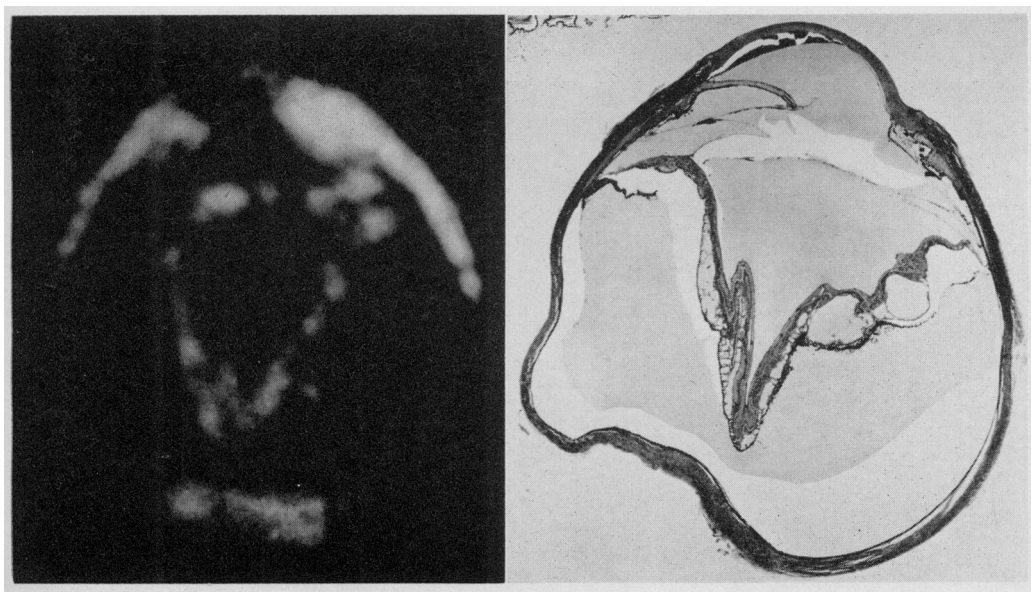

Figure 15

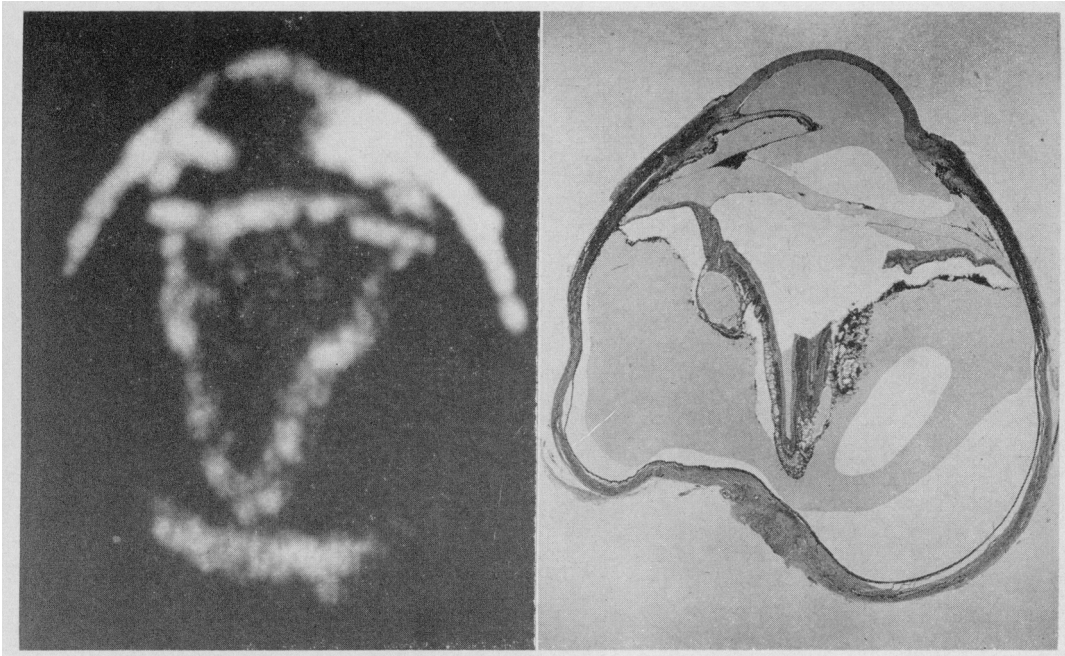

Figure 16

orrhage from vitreous hemorrhage with retinal detachment are the diffuseness and lack of structure of vitreous hemorrhage and the faintness of the echo. These points are well demonstrated in Figure *22*.

This is an ultrasonogram of an aphakic patient who tore off his bandage and stuck his finger into his eye on the sixth postoperative day. A massive vitreal hemorrhage resulted, which totally obscured the fundus. The patient was referred for a determination of the extent of injury to his eye. On the basis of the ultrasonic findings of only a vitreous hemorrhage, a

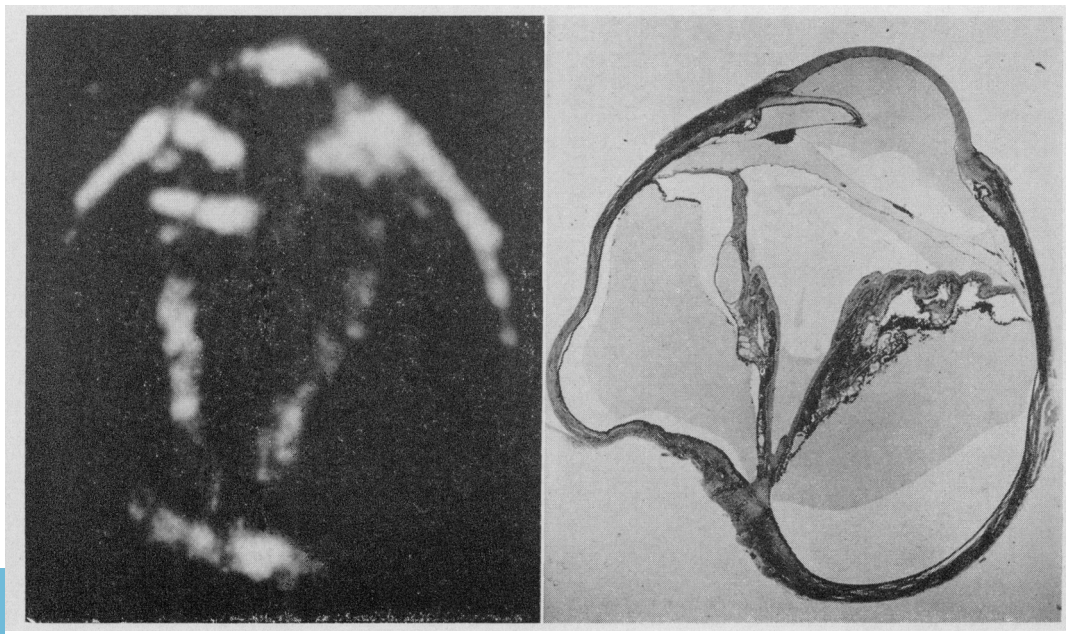

Figure 17

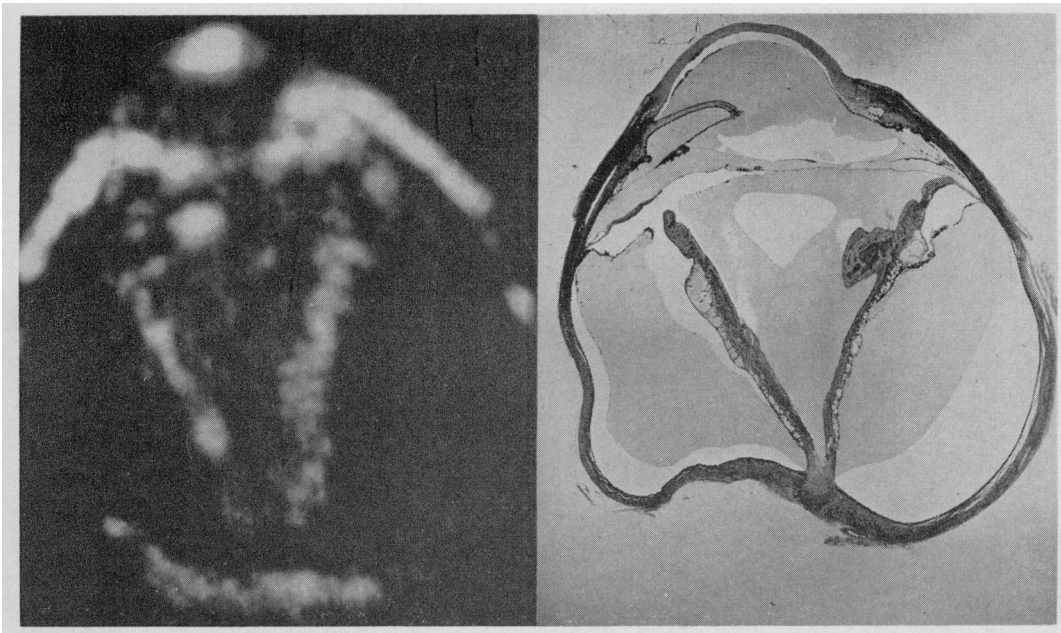

Figure 18

favorable prognosis was rendered. This was subsequently borne out as the vitreous cleared.

Tumors. Another major problem in diagnosis of retinal detachment is the exclusion of a tumor as the primary etiological agent.

Figure 23 shows an eye that was enucleated because of a melanoma of the ciliary body, secondary glaucoma, and cataract. A tumor of the ciliary body was diagnosed because of scleral pigmentation near the tumor site, a pigmented mass visible gonioscopically in the angle and by transillumination.

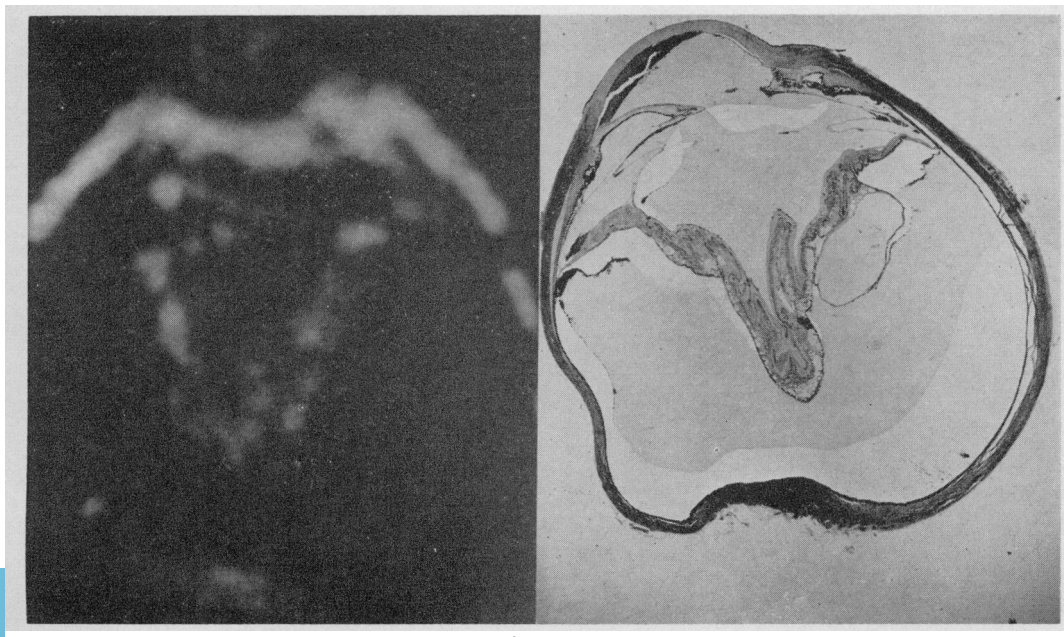

Figure 19

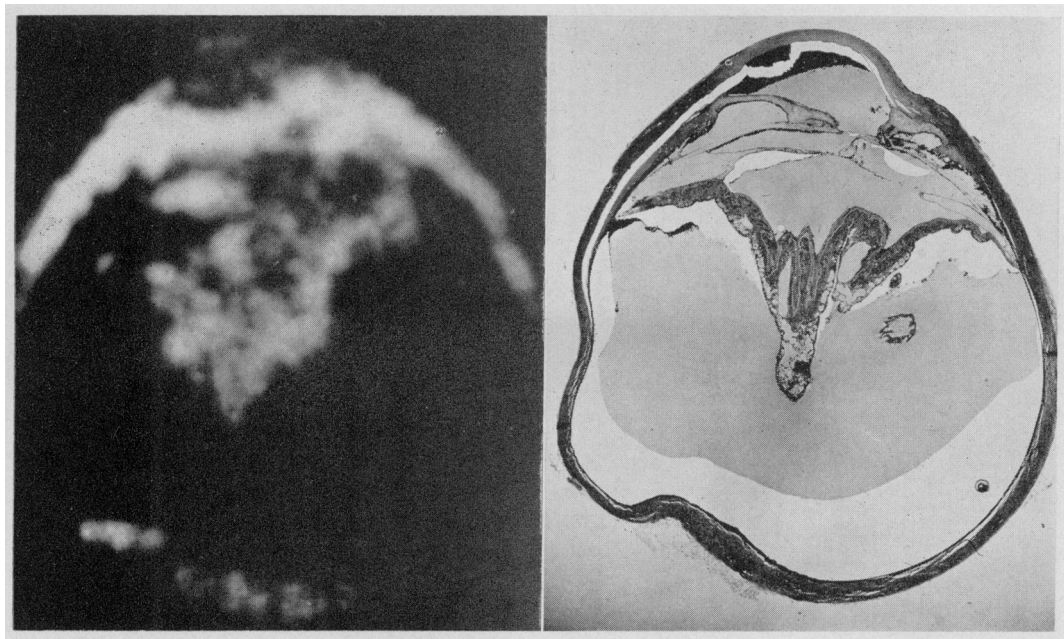

Figure 20

The diagnosis could be made in this instance without the ultrasonic locator because of the anterior location of the tumor. Had the tumor been more posteriorly located, it could not have been diagnosed with certainty prior to the removal of the cataract, as direct light visualization of the tumor would have been impossible. Radioisotope studies would have added little, as the Geiger counter cannot be placed over lesions near the posterior pole.

Despite the translucency to light caused by the cataract, there is no interference with sonic visualization of the anterior portion of the eye and even of the posterior pole.

Figures 24 to 31 are serial ultrasonograms of this eye. When these figures of the eye containing the tumor are compared with an ultrasonogram of a normal human eye (Fig. 32), one may see that the tumor

Figure 21

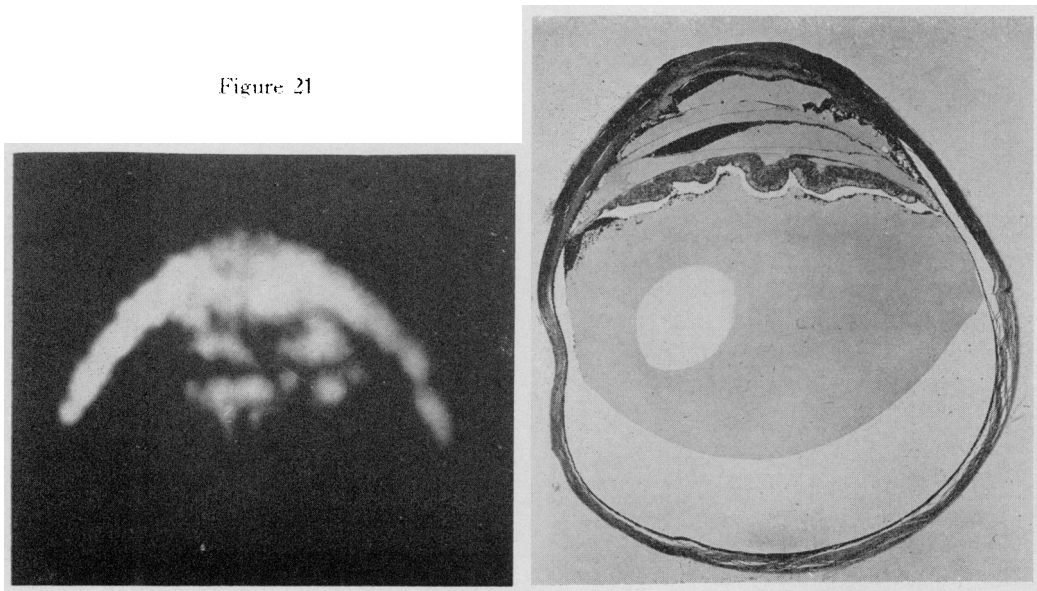

Figure 22

Fig. 22.—Ultrasonogram of an aphakic e

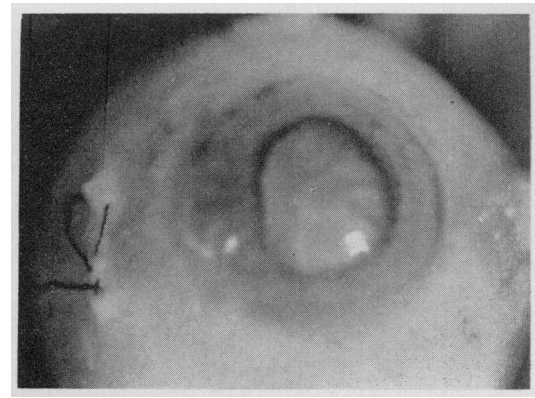

Figure 23

with a massive vitreous hemorrhage. Note the faintness of the echo as well as its random distribution.

Fig. 23.—Gross appearance of eye containing melanoma of the ciliary body. (Patient of Dr. Algernon B. Reese.)

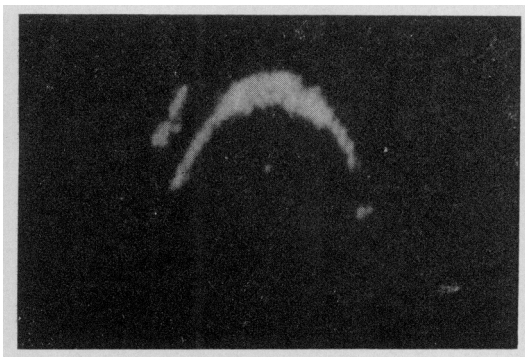

Figure 24

Fig. 24.—Figures 24 to 31 show serial ultrasonic tomograms through an eye containing a

Figure 25

melanoma of the ciliary body, shown in Figure 23. The posterior pole of the eye is visualized in Figures 29, 30, and 31 despite the dense cataract.

echo from the ciliary body tumor is absent in the latter.

Figure 24 is taken above the level of the tumor, figure 31, below. The sonic tomograms are again in a coronal-sagittal plane.

The remainder of the eye is clear of the tumor. This interpretation was confirmed by the histopathological section (Fig. 33).

Despite the cataract, the posterior portion of the eye is visualized. Sections of

Figure 26

Figure 27

Figure 28

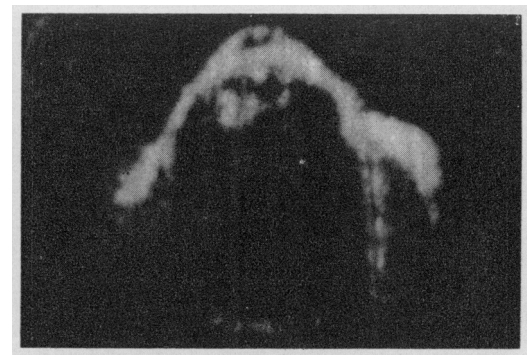

Figure 29

Figure 30

Figure 31

Fig. 32.—First known ultrasonogram of a human eye, at 15 mc. *1*, cornea; *2*, anterior chamber; *3*, iris; *4*, lens; *5*, anterior sclera; *6*, vitreous; *7*, posterior sclera.

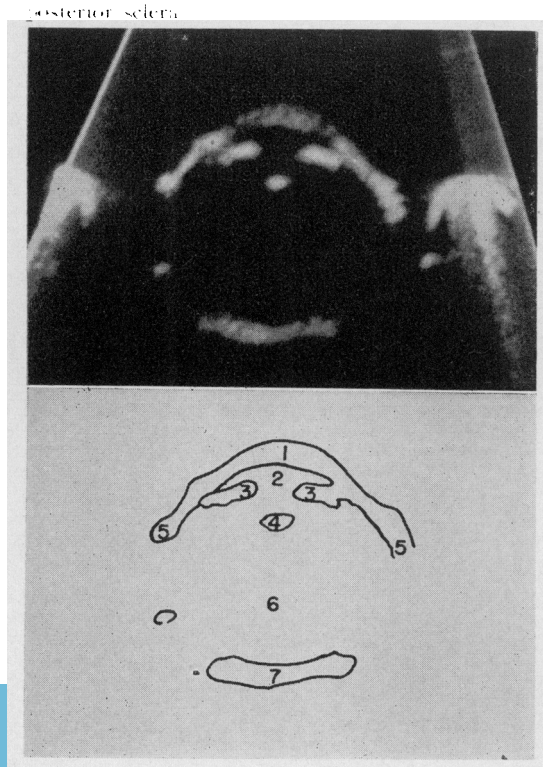

Figure 33

the sclera cannot be visualized with the present equipment without rotating the eye on its vertical axis. A new unit under construction will eliminate this and other defects. All of the eye can be visualized with the present equipment by having the patient rotate his eye. Thus, intraocular tumors at all depths may be visualized if they are larger than 1 mm. in size. This is independent of their response to radioisotopes.

Ultrasonographic interpretation of tumors is limited for the present to the recognition of an echo from an abnormal site.

All the factors which determine the strength of the echo have been determined and will be reported. Since the many variables can now be controlled, and corrected, a study has been initiated which will decide whether there is a difference between the type of echo from malignant and from benign tumors. The echos from foreign bodies are so much stronger than tissue echos that these can easily be distinguished.

Intraocular Foreign Bodies. The next figure (Fig. 34) demonstrates this point.

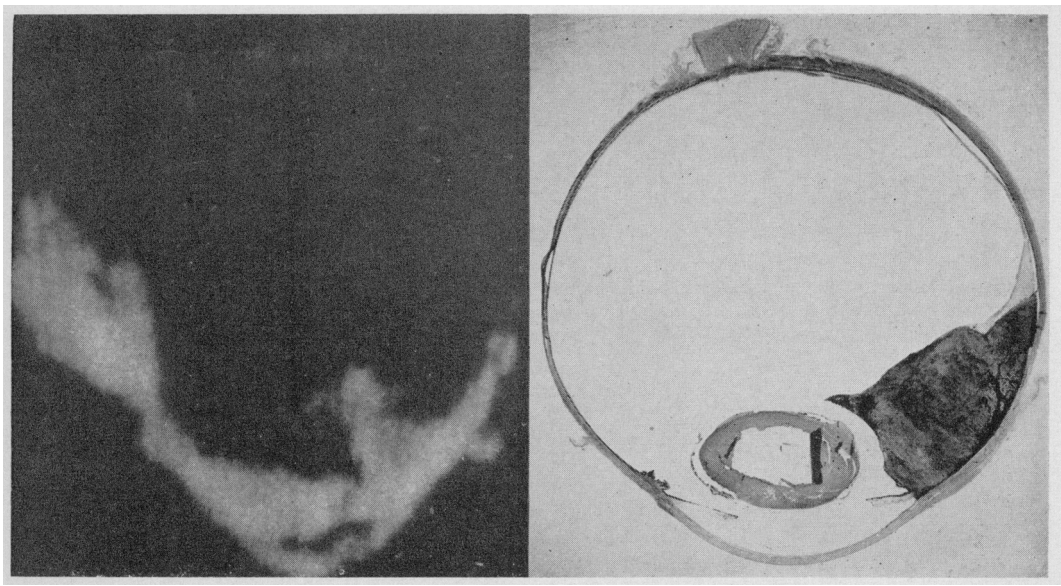

Fig. 33.—Histopathological section of eye in Figure 23, and an ultrasonogram through approximately the same area.

A piece of wood has been inserted into the vitreous of the eye. Although the wood cannot be distinguished on the x-ray, it stands out on the ultrasonogram.

Penetrating foreign bodies frequently will cause hemorrhage as well as retinal detachment. To determine if such a foreign body could be visualized in the presence of a vitreous hemorrhage, blood was injected into the vitreous of this eye (Fig. 35*A*). At maximum sensitivity the foreign body is obscured by the intravitreal blood. However, when the sensitivity of the system is reduced the echos from blood and tissue are, by comparison, so weak that they disappear and only the echo from the wood remains visible (Fig. 35*C*). Thus, radiolucent intraocular foreign bodies may be

Fig. 34.—Comparison of the gross (*A*), x-ray (*B*), and ultrasonic (*C*) appearance of an eye containing a piece of wood in the vitreous. The arrow on the ultrasonogram points to the sonic image of the wood. It is invisible to the x-ray. The precise position of the foreign body as to depth and azimuth may be found directly by the ultrasonic locator.

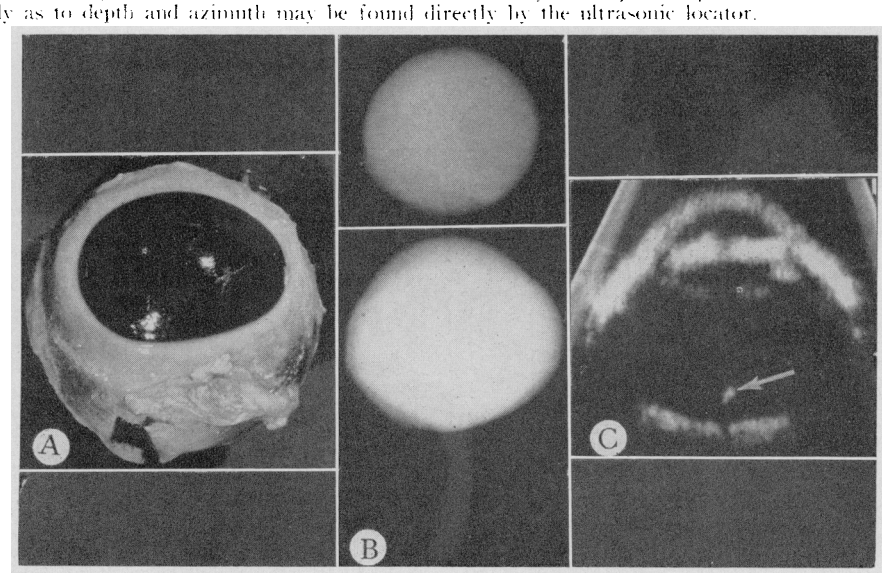

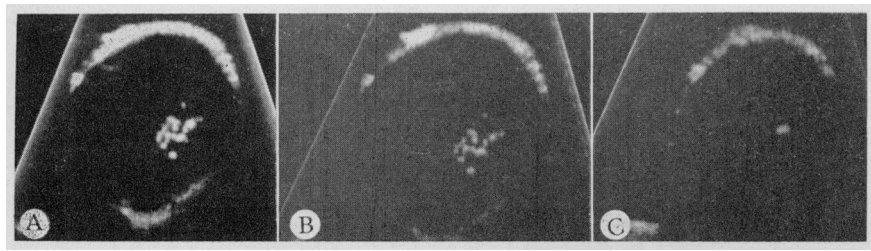

Fig. 35.—The appearance of blood and wood in the vitreous (the eye is viewed laterally through sclera). *A*, viewed with the full-strength transmitted sound beam. *B*, partially attenuated transmitted sound beam. *C*, attenuation of transmitted beam is increased to point at which the echoes from blood and the posterior surface of the eye disappear but the wood remains visible, thus permitting localization of the wood in the presence of blood in the vitreous.

Fig. 36.—Methods of visualizing and locating radiolucent intraocular foreign bodies with use of the combined radar and amplitude-modulated oscilloscope. *A*, measurement of the distance in relation to the major structure of the eye on the A, or amplitude-modulated, scope. Note that a strong foreign-body echo is interposed between the iris and rear-surface echoes. The change in the position of the rear-surface echo is due to the placement of the foreign body in a shorter portion of the eyeball. *B*, azimuth or angular position is determined by measuring the angular displacement of the transducer on a protractor. *C*, appearance on the radar scope when range markers are inserted. Depth can also be measured by calibrating the range markers.

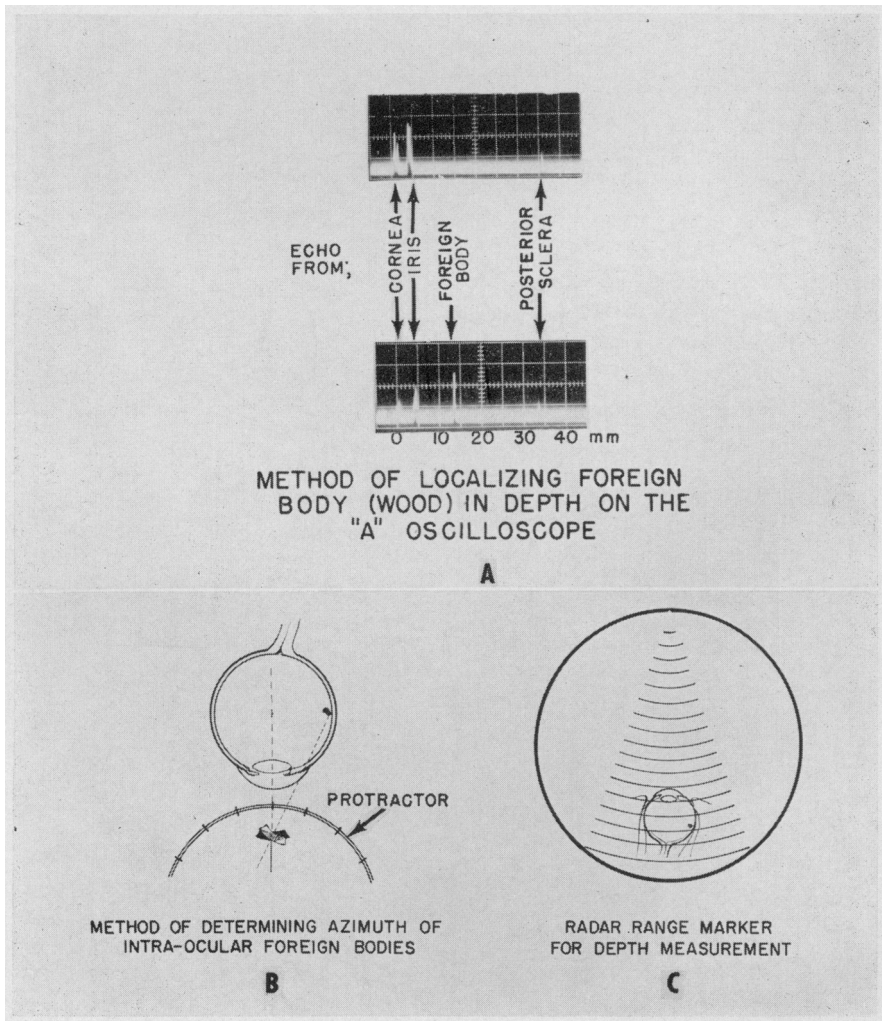

localized, even in the presence of an opaque refractive media and hemorrhage.

Differential Diagnosis Between Vitreous Exudate and Hemorrhage and Between Retinal Detachment, Tumor, and Foreign Body.—Vitreous exudates lack a definitive outline. They are represented by a weak, diffuse, migrating echo (Fig. 22).

Retinal detachments may show similar characteristics, because of associated vitreous opacities, but at some point a strong definitive tissue echo will be located. The strong echo tends to be transient and to shift with the undulation of the retinal folds.

Tumors yield constant strong tissue echos which may be traced by serial tomography to the site of origin or base of the tumor.

The echos from foreign bodies are so strong that they remain after all the tissue echos have been eliminated by attenuation.

Foreign-Body Localization.—The exact depth and azimuth of a foreign body may be determined without any markers on the surface of the eye or in the tissue depth. This is accomplished by calibrating in advance the distances along the trace line (Fig. 36*A*) or by electronically inserting marker points which have also been calibrated. The azimuth is determined by stopping the scanning head when the foreign body is seen and noting the angular direction of the transducer to the foreign body on a protractor scale (Fig. 36*C*).

Summary

The use of pulsed ultrasonic reflection techniques permits direct highly resolved visualization of soft tissues and radiolucent materials, without the use of contrast media. Foreign bodies may be localized without markers in the presence of opaque media. Tumors may be visualized regardless of their position or their selective response to radioisotopes. Criteria for the differential diagnosis of intraocular tumors, retinal detachment, and vitreous hemorrhages, despite the presence of light-opaque media, have been formulated.

Exposure to ultrasonic energy at the levels used in this device is completely safe. The ultrasonograms included in this paper are the equivalents of the first x-rays and should be evaluated in that light. Improvements in equipment will yield far-superior films, and experience, far-wiser interpretations.

Mr. Carl Klammer, of the Special Devices Center, Office of Naval Research, helped during the initial assembly of the equipment. The Department of the Navy and Air Force lent electronic equipment. Dr. Douglas H. Howry and Mr. Jerry Posekany, of Automation Industries, Boulder, Colo., assisted in the design of the transducers.

333 King. St.

REFERENCES

1. Keskey, G. R., and Letsch, W. R.: Retrobulbar Air Injection with Planigraphy, A. M. A. Arch. Ophth. 56:248-256 (Aug.) 1956.

2. Walsh, F. B., and Smith, G. W.: The Ocular Complications of Carotid Angiography: The Ocular Signs of Thrombosis of the Internal Carotid Artery, J. Neurosurg. 9:517-537 (Sept.) 1952.

3. Dunphy, E. B.: Radioactive Isotopes in Ophthalmology: The Charles H. May Memorial Lecture, Am. J. Ophth. 43:857-865 (June) 1957.